

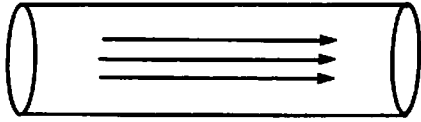
Two Phase Flow of Hot Plastic Through a Cold Mould

INTRODUCTION

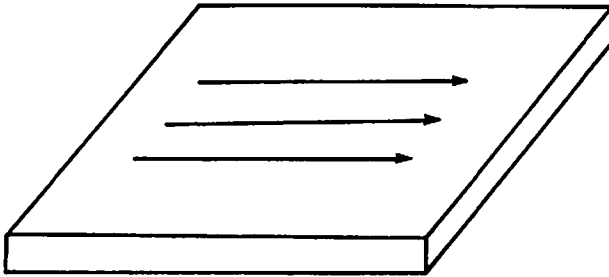
Moldflow Pty Ltd develops and markets CAD software for the plastics industry. They presently have a number of packages which assist in the design of injection moulded products. Some of these are based on a finite difference/finite element model of the coupled flow and heat transfer processes which take place as hot molten plastic is forced under pressure into a cold mould. These models however often require considerable computational effort, particularly for complex geometries. The question Moldflow posed to the Mathematics in Industry Study Group was what could be said about these processes using only a "bare hands" approach (that is, without relying on any significant computing). A particular topic of interest to Moldflow was the growth in thickness of the solid skin as molten plastic flows through a cold mould.

Three geometric configurations were identified as being amenable to some form of analysis. These are shown in Figure 1 and correspond to flow through a long cylindrical tube, plane flow through a slab, and radial flow in a circular disc. These configurations have in common the property that they are two dimensional, with one of these dimensions corresponding to a "slow" coordinate (in the flow direction), whilst the other is a "fast" coordinate (across the flow). Here "fast" and "slow" are meant to indicate the relative rates of change of the various flow parameters (fluid velocity, temperature) in the two coordinate directions. For instance, the midstream fluid temperature is typically of the order of 200 °C falling to a mould wall temperature of say 30 °C in a few millimetres across the flow. On the other hand, the decay in the direction of flow is an order of magnitude slower than this.

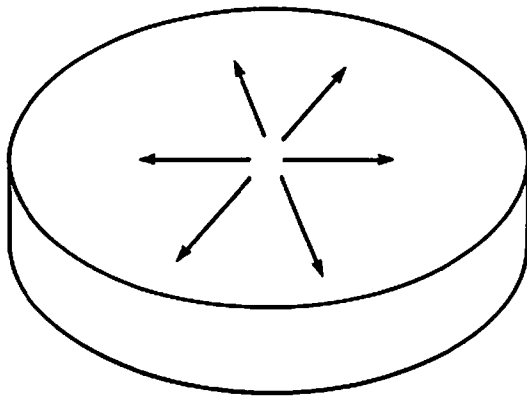
The method of analysis for these three configurations is essentially the same, and for convenience in this report we shall only consider the slab, or Cartesian, case. We shall also restrict our attention to the steady state problem. That is, we suppose that sufficient time has elapsed for any transients in velocity, temperature, skin thickness, etc., associated with the filling process to have settled down, and that all quantities are now time independent.



cylindrical geometry



slab geometry



radial geometry

Figure 1: The various geometries that can be modelled.

CARTESIAN STEADY STATE MODEL

Governing Equations

The model supposes that $\frac{dh}{dx} \ll 1$. This allows us to locally neglect the “slow” variation of h with x , and so all the governing momentum and energy balance relations can be formulated as if the fluid channel width is (locally) constant. (This kind of approach is common in a number of other applications, for instance, lubrication theory.) More precisely, consider a fluid channel of thickness $2h$ (regarded as constant for the moment) as shown in Figure 2.

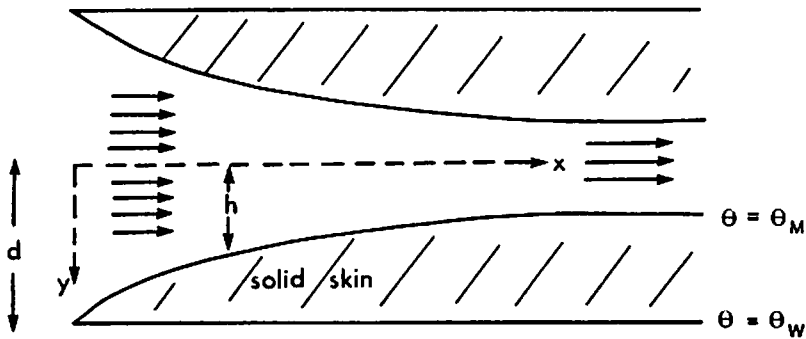


Figure 2: Cross section through a slab in the flow direction. (We suppose that $\frac{dh}{dx} \ll 1$.)

Assuming unidirectional flow, and neglecting any compressibility effects, the equations expressing two-dimensional momentum balance are

$$p_{,x} = (\mu u_{,y})_{,y} \tag{1}$$

$$p_{,y} = 0 .$$

This represents a balance between the pressure gradient which is driving the

flow, and the viscous forces acting within the fluid.

Energy balance within the fluid can be described by

$$\rho c u \theta_{,x} = (k \theta_{,y})_{,y} + \mu (u_{,y})^2 . \quad (2)$$

The left hand side of this equation accounts for convective heat transfer, while the terms on the right hand side represent conduction and viscous dissipation within the fluid. Within the solid skin we only consider heat conduction in a direction through the thickness of the slab, so that

$$(k_s \theta_{,y})_{,y} = 0 \quad (3)$$

is the appropriate governing equation. There must also be a heat balance at the solid-fluid interface. This requires

$$\theta(\text{solid}) = \theta(\text{fluid}) = \theta_M \quad (4a)$$

$$k_s \theta_{,y}(\text{solid}) = k \theta_{,y}(\text{fluid}) . \quad (4b)$$

(Note that implicit in (3) and (4) is the assumption that an interface, and thus a solid skin, actually exists. That is, $h < d$.)

We cannot however completely neglect the variation of h with x . Whilst it is permissible to neglect any "slow" variation of h in formulating the above local balance relations, such variations in h must nonetheless be accounted for in some global sense. We do this by specifying a fixed volumetric flow rate q which may be related to the velocity u by

$$\int_0^h u \, dy = \frac{q}{2w} = Q . \quad (5)$$

The goal now is to solve (1)-(5), and so find

$$u = u(x,y) , \quad \theta = \theta(x,y) , \quad p = p(x) , \quad h = h(x)$$

in terms of the various material properties and the flow parameters Q and d . In general an exact, analytic solution in a tractable form is not possible, even in the case of constant material properties. However a number of approximate techniques can be usefully employed. We shall illustrate one such approach for the case of a Newtonian fluid (that is, all material properties constant).

An Approximate Solution Technique (Newtonian Fluid)

We begin by a priori assuming that within the fluid u and θ take the forms

$$u(x,y) = u_0(x) \left(1 - \phi \left(\frac{y}{h} \right) \right) \quad (6)$$

$$\theta(x,y) = \theta_0(x) \left(1 - \psi \left(\frac{y}{h} \right) \right) + \theta_M$$

where u_0 , θ_0 , ϕ and ψ are to be determined. The symmetry condition

$$u_{,y} = \theta_{,y} = 0$$

at $y = 0$ implies that

$$\psi'(0) = \phi'(0) = 0 ,$$

whilst the boundary condition (4a) at $y = h$ means

$$\psi(1) = \phi(1) = 1 .$$

These give velocity and temperature profiles across the flow as shown in Figure 3. Physically, (6) corresponds to taking the y -profiles of u and θ to be of a fixed shape, with only their amplitudes varying along the flow direction x . For the moment we suppose that the profile functions ϕ and ψ are known (we shall discuss some choices for them later), and address the problem of determining the amplitudes u_0 and θ_0 along with $p = p(x)$ and $h = h(x)$. This will be done by applying the following versions of (1) and (2) which have been averaged over the half thickness $0 < y < h$,

$$\int_0^h p_{,x} dy = \int_0^h (\mu u_{,y})_{,y} dy$$

$$\int_0^h \rho c u \theta_{,x} dy = \int_0^h (k \theta_{,y})_{,y} dy + \int_0^h \mu (u_{,y})^2 dy .$$

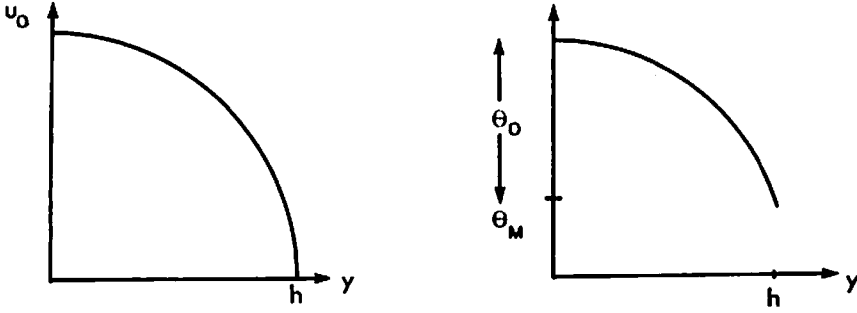


Figure 3: Velocity and temperature profiles in the fluid.

Substituting the assumed forms for u and θ into these gives after a little algebra

$$h \frac{dp}{dx} = -\mu \frac{u_0}{h} \phi'(1) \quad (7)$$

$$\rho c u_0 h \lambda_1 \frac{d\theta_0}{dx} = -\frac{k\theta_0}{h} \psi'(1) + \mu \frac{u_0^2}{h} \lambda_2 \quad (8)$$

where $\phi'(1)$, $\psi'(1)$,

$$\lambda_1 = \int_0^1 (1 - \phi(\xi))(1 - \psi(\xi)) d\xi,$$

and

$$\lambda_2 = \int_0^1 (\phi'(\xi))^2 d\xi$$

are (non-dimensional) numeric constants depending only on the shape of the profile functions ϕ and ψ . (In evaluating $\theta_{,x}$ we have neglected the variation of h with x in accord with our earlier supposition that $\frac{dh}{dx} \ll 1$.) From (5) we find

$$u_0 h \lambda_3 = Q,$$

where

$$\lambda_3 = \int_0^1 (1 - \phi(\xi)) d\xi.$$

Using this to eliminate u_0 from (7) and (8) yields

$$\frac{dp}{dx} = - \frac{\mu Q}{h^3} \left[\frac{\phi'(1)}{\lambda_3} \right] \quad (9)$$

$$\rho c Q \frac{\lambda_1}{\lambda_3} \frac{d\theta_0}{dx} = - \frac{k}{h} \psi'(1) \theta_0 + \mu Q^2 \frac{\lambda_2}{\lambda_3^2} \frac{1}{h^3}. \quad (10)$$

Turning now to the solid, (3) and (4a) immediately give (for the case of a constant solid conductivity k_s) a linear temperature profile

$$\theta = \theta_M + (\theta_W - \theta_M) \frac{y-h}{d-h}$$

across the solid. Using this in (4b) we find

$$k_s \frac{(\theta_W - \theta_M)}{d-h} = - \frac{k\theta_0}{h} \psi'(1),$$

that is

$$\theta_0 = \frac{k_s}{k\psi'(1)} (\theta_M - \theta_W) \frac{h}{d-h}. \quad (11)$$

Substituting (11) into (10) we may eliminate θ_0 and obtain an ordinary differential equation for $h = h(x)$. By introducing the nondimensional quantities

$$H = \frac{h}{d},$$

$$X = \frac{x}{d} \left[\psi'(1) \frac{\lambda_3}{\lambda_1} \right] \frac{k}{\rho c Q},$$

and

$$\gamma = \left[\frac{\lambda_2}{\lambda_3^2} \right] \frac{\mu Q^2}{d^2 k_s (\theta_M - \theta_W)},$$

this equation may be conveniently written

$$\frac{dH}{dX} = -(1-H) + \gamma \frac{(1-H)^2}{H^3}. \quad (12)$$

The corresponding nondimensional versions of (9) and (11) are

$$\frac{dP}{dX} = -\frac{1}{H^3} \quad (13)$$

$$T = \frac{H}{1-H} \quad (14)$$

where

$$P = p \left[\frac{\lambda_3^2 \psi'(1)}{\lambda_1 \phi'(1)} \right] \frac{d^2 k}{\rho c \mu Q^2}$$

$$T = \theta_0 [\psi'(1)] \frac{k}{k_s (\theta_M - \theta_W)}.$$

Plots of solution curves of (12)-(14) for a selection of values of the parameter γ are shown in Figures 4a, 4b and 4c. These particular curves correspond to the initial conditions

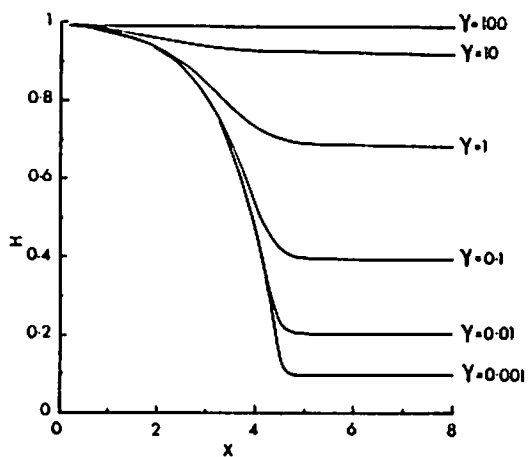
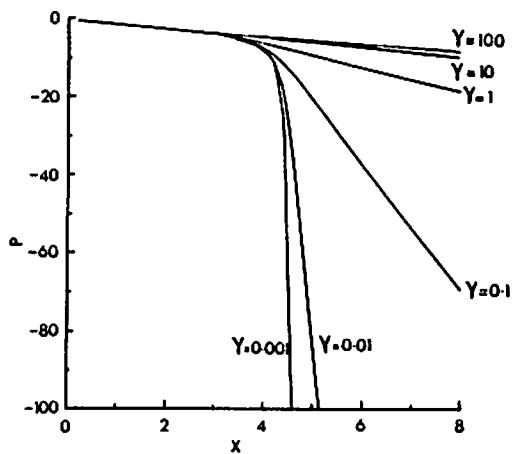
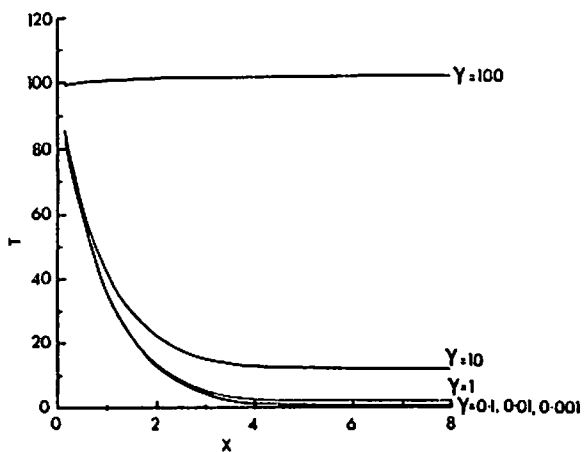
$$H(0) = 0.99, \quad P(0) = 0.0.$$

However, as (12) and (13) do not explicitly contain X or P , the choice of origins for X or P is arbitrary (only differences in X and P are physically significant). The solution curves for other initial conditions can therefore be obtained by simply moving the origin of the X axis in all plots so that the H vs. X plot gives the required value for $H(0)$, and then adjusting the origin of the P axis in the P vs. X plot to give the correct initial value to P .

Notice that $H = 1$ is an unstable equilibrium point of (12). The other equilibrium point is given by the solution of the algebraic equation

$$\frac{H^3}{1-H} = \gamma$$

which always has a unique root in the range $0 < H < 1$ for $\gamma > 0$. This equilibrium point is a stable attractor for all solutions starting in the range $0 < H < 1$ (which, of course, are the only solutions which make sense physically

Figure 4a: Channel Width H .Figure 4b: Pressure drop P .Figure 4c: Temperature T .

in this application). This is readily seen in Figure 4(a), where all the H vs. X curves reach their equilibrium values by about $X = 5$.

Hitherto we have not been specific about the profile functions ϕ and ψ . Notice however that the particular choice of such profiles will only change the numeric constants enclosed within [...] in the above definitions of X, P, T and γ . The qualitative character of the solutions is thus essentially independent of the particular profiles. In fact, the above analysis introduces a number of important dimensionless groups and suggests which aspects of the process they may govern. The group

$$\frac{k}{\rho c Q}$$

would seem to determine how rapidly the skin thickness reaches its equilibrium value, while

$$\frac{\mu Q^2}{d^2 k_s (\theta_M - \theta_W)}$$

governs the magnitude of this thickness.

A simple class of profiles would be given by

$$\phi(\xi) = \xi^n, \quad \psi(\xi) = \xi^m$$

for n, m positive integers say. As n and m increase these profiles become more bluff, and in the limit as $n, m \rightarrow \infty$ a slug flow profile is obtained.

The proper choice of velocity profile is relatively straight forward for a Newtonian fluid as (1) can be solved directly to give the usual Hagan-Poiseuille quadratic profile

$$u = - \frac{P_x h^2}{2\mu} \left(1 - \left(\frac{y}{h} \right)^2 \right). \quad (15)$$

The case of the temperature profile is not as clear, due to the presence of the convective term on the left hand side of (2). One possibility is to use the "equilibrium" profile, that is, the profile that would apply were all the x variation dropped from (2). This is perhaps not an unreasonable choice since, as was mentioned in the introduction, we are dealing with a situation in which there is a "slow" variation of u and θ in the x -direction, in contrast to a

“fast” variation in the y -direction. If the x dependence is neglected, then (2) becomes

$$k\theta_{,yy} + \mu(u_{,y})^2 = 0 .$$

Using (15) to eliminate $u_{,y}$ we find after some calculation

$$\theta = \frac{p_x^2 h^4}{12k\mu} \left(1 - \left(\frac{y}{h} \right)^4 \right) + \theta_M .$$

That is, a quartic profile.

A possible extension of the technique outlined here is to assume the following forms for u and θ in place of (6)

$$u(x,y) = \sum_{i=1}^N u_i(x) \left(1 - \phi_i \left(\frac{y}{h} \right) \right)$$

$$\theta(x,y) = \sum_{i=1}^L \theta_i(x) \left(1 - \psi_i \left(\frac{y}{h} \right) \right) + \theta_M$$

where $N, L > 1$. In this case one will need to satisfy not only averaged versions of (1) and (2), but also an appropriate number of moments across the y -direction of (1) and (2). This will lead to a system of ordinary differential equations which will need to be solved to determine $h = h(x)$, rather than the single ordinary differential equation (12) as in the present case. This will necessitate more computational effort.

Non-Newtonian Case

In principle, the technique outlined above could also be applied in the case of a non-Newtonian fluid. However, in general the problem will likely become computationally intensive. The special case of a “power law” fluid with

$$\mu = A(u_{,y})^\alpha$$

(A, α constants) can be handled quite easily. However once a temperature dependence is introduced into μ , as in the commonly accepted

$$\mu = A(u, y)^\alpha \exp(B\theta)$$

(A, B, α constants) then (1) and (2) become coupled, and little progress would seem possible without substantial computation.

Selected Notation

p	pressure
P	nondimensional pressure
u	fluid velocity
μ	viscosity
θ	temperature
T	nondimensional temperature
θ_M	melting temperature of plastic
θ_W	wall temperature of mould
k	thermal conductivity of molten plastic
k_s	thermal conductivity of solid plastic
ρ	density
c	specific heat
h	fluid channel half-width
d	slab half-thickness
H	nondimensional channel half-width
q	volumetric flow rate
w	slab width
Q	(see (5))
ϕ, ψ	nondimensional velocity, temperature profile functions
ξ	nondimensional dummy variable running over range 0 to 1
ϕ', ψ'	derivatives with respect to ξ
$\lambda_1, \lambda_2, \lambda_3$	nondimensional numeric constants
γ	nondimensional parameter (see (12))

x	cartesian coordinate along the flow
y	cartesian coordinate across slab thickness
X	nondimensional version of x (see (12))
\cdot_x	differentiation with respect to x
\cdot_y	differentiation with respect to y